Anal. Chem. **1998,** *70,* 3191−3197

Laser-Induced Fluorescence of Perylene in a Microparticle Suspension Environment

Batya Horowitz, Vladimir V. Gridin, Valery Bulatov, and Israel Schechter*

Department of Chemistry, Technion—Israel Institute of Technology, Haifa 32000, Israel

Laser-induced fluorescence (LIF) is one of the most sensitive techniques for analysis of traces of polycyclic aromatic compounds in liquids. Application of this method to on-line monitoring requires solution of problems related to the presence of particulate materials. Thus, understanding the analytical effects associated with the suspension of microparticles is of considerable importance for both environmental and industrial applications. Here, LIF of perylene in acetonitrile solutions was studied for different light-scattering/-absorbing microparticle matrixes. With increasing suspension mass of efficiently light absorbing black-colored particles, the intensity of the associated LIF signals was found to obey an apparently exponential decrease. Their white-colored counterparts, however, have initially produced a sizable, ∼20%, signal increase of the respective LIF responses. An exponential decrease then became predominant, too. A model that explains the observations in terms of absorption and scattering coefficients is developed and examined. The quantitative effect of the particulate mass is correctly reproduced by the model, as well as the laser wavelength dependence. A possible application of a calibrating algorithm is addressed.

Specific demands of in situ, on-line, and remote analytical monitoring of various environmental targets of interest impose a prerequisite of elimination or, at least, serious minimization of the associated sample preparation routines. Spectroscopic testing of dissolved organic pollutants, hence, is expected to be carried out in complex media containing different types of microparticles, particle clusters, or muddy (opaque) coagulants. Similar problems are faced when on-line analysis is required for process control in several industrial applications. Reflectance spectroscopy of turbid materials has been investigated; however, very little is known about the analytical effects of microparticle suspensions upon laser-induced fluorescence signals.[1,2]

There exists an ever-growing need for reasonably low cost, yet analytically reliable and simple in their operational mode, portable field kits with remote control access to data acquisition and processing. Laser-based spectroscopic tools, by and large, supply such needs.[3−5] The laser-induced fluorescence (LIF) analytical method[6,7] is, by any means, one of the most sensitive and widely employed. Thus, the investigation of LIF analysis in microparticle suspensions is of considerable importance.

Pulsed lasers, optical fibers, and various waveguides have largely increased the applicability of the method, especially when its time-resolved and remote control potential are fully utilized.[8−10] New low-cost PC plugged-in optical fiber spectrometers and solid-state lasers enable construction of compact and portable LIF setups. The availability of frequency doublers and tunable dye lasers makes its application highly selective and very efficient in trace detection techniques. Thus, the LIF technique has already been coupled to numerous detection systems and analytical instruments in mass spectroscopy, chromatography, plasma ionization, laser-induced breakdown spectroscopy, etc.[11−19]

In all the above applications, homogeneity of the medium (on the molecular scale) is assumed. Nevertheless, most real samples are actually not homogeneous, due to the presence of hydrosols or microparticles. Proper filtration and sample pretreatment is not possible in many on-line applications. It is expected that these suspended materials have an effect on the quantification of the analyzed fluorescing compounds in the liquid. It is also expected that the nature of these effects depends on the nature of the microparticles and on their concentration. Thus, a characterization of these effects and an understanding of their nature may result in a possible calibration procedure that can compensate for the presence of microparticles, without any physical filtration.

We report some of the major effects of suspended micromaterials on LIF signals. Different light-scattering/-absorbing

(1) Schmitt, J. M.; Kumar, G. *Appl. Spectrosc.* **1996**, *50*, 1066−1073.
(2) Schmidt, W. *Trends Anal. Chem*. **1993**, *12*, 74.
(3) Svanberg, S. *Phys. Scr*. **1988**, *T23*, 281.
(4) Svanberg, S. *Appl. Phys. B* **1988**, *B46*, 271.
(5) McManus, K.; Yip, B.; Candel, S. *Exp. Therm. Fluid Sci*. **1995**, *10*, 486.
(6) Letokhov, V. S. *Laser Analytical Spectrochemistry*; Adam Hilger: Bristol, PA, 1986.
(7) *Laser Applications to Chemical Analysis*; 1990 Technical Digest Series; Optical Society of America: Washington, DC, 1990; Vol. 2.
(8) Norris, J. O. W. *Analyst* **1989**, *114*, 1359−1371.
(9) Fujiwara, K.; Ito, S. *Trends Anal. Chem*. **1991**, *10*, 184−90.
(10) Brown, R. S.; Brennan, J. D.; Krull, U. J. *Microchim*. **1994**, *50*, 337−350.
(11) Haugen, G. R.; Lytle, F. E. *Anal. Chem*. **1981**, *53*, 1554.
(12) Hughes, K. D.; Huber, D. M.; Lytle, F. E. *Anal. Chem*. **1989**, *61*, 1656.
(13) Azimi, N. T.; Huber, D. M.; Whitaker, J. E.; Haugland, R. P.; Lytle, F. E. *Appl. Spectrosc*. **1990**, *44*, 400.
(14) Fasset, J. D.; Travis, J. C. *Spectrochim. Acta* **1988**, *43B*, 1409.
(15) Kim, H.-B.; Hayashi, M.; Nakatani, K.; Kitamura, N.; Sasaki, K.; Hotta, J.-I.; Mashuhara, H. *Anal. Chem*. **1996**, *68*, 409−414.
(16) Diebold, G. J.; Zare, R. N. *Science* **1977**, *196*, 1439.
(17) Diebold, G. J.; Karny, N.; Zare, R. N.; Seitz, L. M. *J. Assoc. Off. Anal. Chem*. **1979**, *62*, 564.
(18) Omeneto, N.; Winefordner, J. D. In *Inductively Coupled Plasmas in Analytical Atomic Spectrometry*; Montaser, A., Golightly, D. W., Eds.; VCH Publishers: New York, 1987; Chapter 9.
(19) Cremers, D. A.; Barefield, J. E.; Koskelo, A. C. *Appl. Spectrosc.* **1995**, *49*, 857.

S0003-2700(98)00046-8 CCC: $15.00
Published on Web 06/18/1998

microparticle matrixes were used. A somewhat unexpected fluorescence signal increase is observed in some of the cases examined. We aimed to establishing principal behavioral patterns in two limiting types of suspensions. These were composed of (a) black-colored, predominantly light-absorbing, and (b) white-colored, merely reflecting microparticle powders. Preliminary results of modeling these effects are provided. LIF was applied here within an experimental arrangement based on portable components, as required in many on-line applications. The results first reported here are correctly fitted within the proposed model; however, a complete or comprehensive presentation of the subject has not been attempted. Thus, this study makes only a first and preliminary contribution to this interesting field.

EXPERIMENTAL SECTION

Sample Preparation and Microparticle Matrixes. Fresh perylene solutions in acetonitrile were routinely prepared for each type of microparticle suspension used here. For simplicity, the results presented here were obtained for a constant perylene concentration of 1.4 ppm. (Experiments at different concentrations were also carried out, leading to similar qualitative results.)

Saturation of the adsorption was then carried through: 2−5 g of microparticle powder was mixed and thoroughly stirred (0.5 h) with 50 mL of the 1.4 ppm perylene solution. This step is very important for materials possessing a large surface area (e.g., graphite and carbon powders), since we want to isolate the optical effects of microparticles, and we have to avoid artifacts due to the low solution volume used. (Otherwise, the addition of unsaturated microparticles to a low-volume solution would cause an artificial reduction of the concentration.) Due to surface quenching effects, the fluorescence contributed by the adsorbed perylene was found to be negligible relative to the figures obtained in this study.

A few hours later, upon completion of particle precipitation, the liquid phase was LIF tested, and the intensity of the perylene characteristic spectrum was looked up for a "perfect match" (within 0.1% spectral reproducibility) with that of the original, as-prepared 1.4 ppm solution. If not, the mixture was then drained off perylene/acetonitrile residual, and another 50 mL of the 1.4 ppm solution was subsequently applied as before. Until the adsorption saturation was reached, we kept repeating the aforementioned procedural steps. Thus, the final solutions had a perylene liquid concentration of 1.4 ppm, while the microparticles were already saturated. The resulting powder was then dried.

Afterward, the adsorption-saturated microparticle powder was used to build up a sequence of suspension samples. In this process, a preset amount of the powder (increased in 20-mg weight portions) was added and thoroughly mixed with 10 mL of as-prepared 1.4 ppm solution. While continuing mechanical stirring and mixing, about 3 mL of resulting suspension was sampled out and poured into a quartz cuvette. The cuvette also contained miniature magnetic stirrers that were kept activated during the LIF data acquisition. The suspensions used were found to be homogeneous (at the scale relevant to the detection system). The research was limited to small enough particles such that the stirring could maintain the homogeneity of the liquid medium.

Materials. For the sample preparation part of this work an analytical grade of acetonitrile (Frutarom Ltd., Haifa, Israel) and 98% perylene (Sigma Ltd.) were used without further purification.

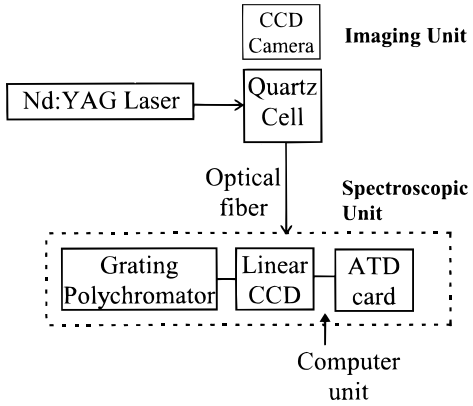

Figure 1. Schematics of experimental arrangement for LIF data acquisition.

Several microparticle powders were used, and their particle size distributions, although certified by the suppliers, were independently cross-referenced and verified by a standard particle size analyzer (Coulter LS230, 0.04−2000 μm): (a) aluminum oxide 99.9%, <10 μm (actually 5 ± 3 μm), Aldrich; (b) aluminum oxide 99.99%, 0.3 ± 0.1 μm, Fluka; (c) silica (SiO_2) 99%, 0.5−10 μm (actually 3 ± 2 μm), Sigma; (d) activated carbon, 6 ± 1 μm, Serva; (e) graphite, 2 μm, Leico Industries.

Experimental Setup. Schematics of the experimental arrangement for LIF acquisition are depicted in Figure 1. For the purpose of LIF analysis, each one of the probes was poured into a quartz cuvette and irradiated by pulses of fourth harmonic generation of a Nd:YAG laser (Minilite, Continuum; 266 nm, 3 mJ in 5-ns pulses at 10 Hz). An unfocused laser beam of 2-mm diameter was used.

Remote detection of LIF signals was obtained in a 90° (laser beam to detector) geometry by means of quartz optical fibers. The observation cone of the fiber (60°) included the whole relevant fluorescence scene into the detected field of view. Fluorescence spectra were obtained by a PC-interfaced linear CCD spectrometer (Ocean Optics) in the 100-ms exposure time mode at 5-nm resolution. Every LIF spectrum presented in the Results and Discussion section is averaged over 40 such LIF events.

Fluorescence Imaging. The fluorescence from the quartz cuvette was directly imaged onto a slow scan cooled CCD camera (Micro-Max, 512 × 512 pixels, Princeton Instruments). Fluorescence light was discriminated from the excitation source by means of optical filters. In this way we obtained two-dimensional fluorescence figures that provided insight into the fluorescence signal increase mechanism.

Environmental Conditions. LIF measurements were conducted under usual laboratory conditions, i.e., room temperature (20 ± 2 °C), ambient air pressure (750 ± 5 Torr) and composition, and ambient laboratory moisture level (65 ± 10%).

Computer Programs. All computer programs for data analysis and model evaluation were written in FORTRAN 77 and compiled by a Power-Station 1 compiler. All codes were run on a PC (Pentium processor).

RESULTS AND DISCUSSION

Physical Grounds. The physical concepts describing the system are simple (although the mathematical treatment is rather

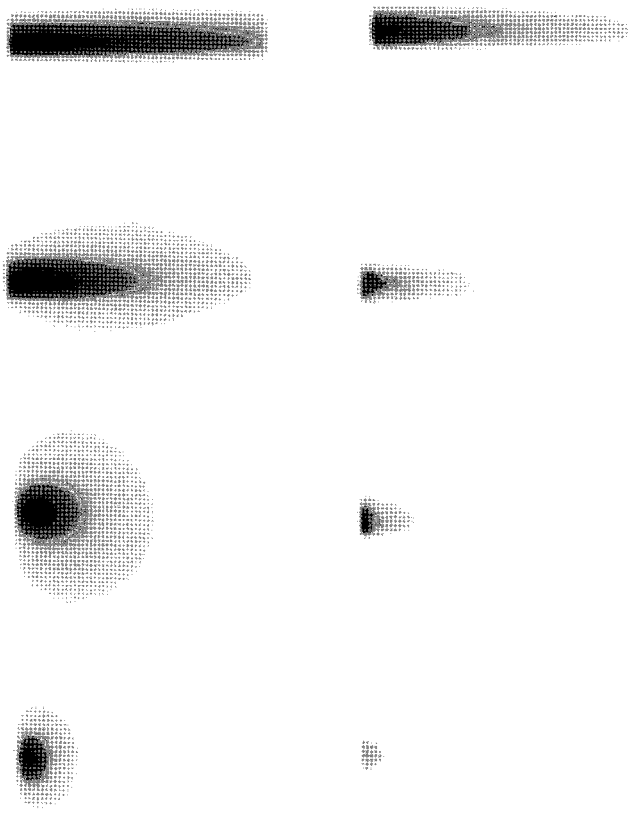

Figure 2. Fluorescence images of microparticle solutions. Black particles (right) and white particles (left). Images correspond to ever-increasing microparticle concentrations (from top to bottom).

complicated). The laser beam is partially absorbed by the fluorescing molecules and partially absorbed by the nonfluorescing microparticles. In addition, a portion of the laser light is scattered by the microparticles. The scattered light can be absorbed (by molecules and by other microparticles) as well as rescattered. Thus, the problem at hand should involve two absorption coefficients (of the fluorescing molecules and of the microparticles) and one scattering coefficient (of the microparticles).

As long as black-colored microparticles are concerned, the scattering coefficient is small, and a composed Beer−Lambert exponential decay of the fluorescence is expected. However, when the scattering coefficient is not negligible (white particles), two additional mechanisms are introduced: The effective laser beam path is elongated, due to the scattering process, resulting in a fluorescence signal increase. Moreover, fluorescence photons, which are spherically emitted, have a larger probability to reach the detector (placed at a 90° configuration). A photon emitted outside the detector collection angle may be scattered and redirected toward the detector. Again, an initial certain fluorescence signal increase is expected; however, it is clear that the asymptotic behavior of the fluorescence as a function of microparticle concentration must reach an apparent exponential decay. At very high concentrations, the excitation light is actually blocked.

The above physical grounds are based on inspection of the fluorescence images of microparticle solutions. Several examples are shown in Figure 2. On the right side, the perylene fluorescence images from solutions containing black-colored microparticles are shown. A series of images of ever-increasing microparticle concentrations (from top to bottom) is given. At low microparticle concentrations, the fluorescence image represents the laser beam passing in the solution. An increase in the microparticle concentration results in absorption of a portion of the laser beam; thus, the fluorescence image becomes shorter. Finally, at very high concentrations (bottom), the laser beam is almost blocked by the microparticles, and only a weak and small fluorescence image is observed.

On the other hand, in the presence of white-colored microparticles, the fluorescence images look quite different (left part of Figure 2). Again, four figures are shown for ever increasing microparticle concentration (from top to bottom). Here, in addition to the blocking of the laser beam by the microparticles, a clear signal increase is observed. It originates from the scattered light, as can be seen by the enlargement of the image in the coordinate perpendicular to the beam. Also in this case, at the limit of very large microparticle concentration, an overall fluorescence decay is observed.

The conclusion from the above images is that a realistic description of the system under consideration must be carried out in at least a two-dimensional plane, so that the fluorescence signal increase can be accounted for. As shown in the next subsection, a single-dimensional model cannot account for the observed fluorescence signal increase.

Theory. The mathematical basis for the treatment of optically nonhomogeneous and nontransparent media dates back to Schuster's differential equations for diffuse scattering materials (1905).[20] These equations were derived for the description of the behavior in a foggy atmosphere of radiation from a star. Later (1948), Kubelka developed a set of useful equations that provide the foundations for many quantitative studies of absorption, reflection, and fluorescence processes of diffuse scattering media.[21] These equations, which were derived for a one-dimensional model, are given below:

$$-\frac{\mathrm{d}i}{\mathrm{d}x} = -(S+K)i + Sj$$
$$\frac{\mathrm{d}j}{\mathrm{d}x} = -(S+K)j + Si \qquad (1)$$

where i is the intensity of light propagating inside the sample in the transmitted direction, j is the intensity of light propagating inside the sample in the backscattered direction, S is the scatter coefficient, K is the absorption coefficient, and x is the distance from the nonilluminated side. These differential equations have been integrated in relation to the phosphorimetry of frozen organic matrixes.[22] We adopt these (mathematically solvable) equations and slightly modify the results to make them applicable to fluorescence in the presence of microparticles, namely $K = \epsilon_c C + \epsilon_m m$, $S = \epsilon_s m$. We obtain

$$i = A(1-\beta)\mathrm{e}^{\alpha\bar{x}} + B(1+\beta)\mathrm{e}^{-\alpha\bar{x}}$$
$$j = A(1+\beta)\mathrm{e}^{\alpha\bar{x}} + B(1-\beta)\mathrm{e}^{-\alpha\bar{x}} \qquad (2)$$

where $\bar{x}$ is the average path length for diffuse reflectance and

(20) Schuster, A. *Astrophys. J.* **1905**, *21*, 1.
(21) Kubelka, P. *J. Opt. Soc. Am.* **1948**, *38*, 448.
(22) Zweidinger, R.; Winefordner, J. D. *Anal. Chem.* **1970**, *42*, 639−637.

$$\alpha = \sqrt{(\epsilon_c C + \epsilon_m m)(\epsilon_c C + \epsilon_m m + 2\epsilon_s m)}$$
$$\beta = \sqrt{\frac{\epsilon_c C + \epsilon_m m}{\epsilon_c C + \epsilon_m m + 2\epsilon_s m}} \quad (3)$$

where ϵ_c is the absorption coefficient of the fluorescing agent, C is its concentration, ϵ_m is the absorption coefficient of the microparticles, m is their concentration, and ϵ_s is the scattering coefficient of the microparticles.

The coefficients A and B are found by the system boundary conditions ($i = i_0$ at $x = 0$, and $j = 0$ at $x = b$) as follows:

$$A = \frac{-i_0(1-\beta)e^{-\alpha\bar{b}}}{(1+\beta)^2 e^{\alpha\bar{b}} - (1-\beta)^2 e^{-\alpha\bar{b}}}$$
$$B = \frac{i_0(1+\beta)e^{-\alpha\bar{b}}}{(1+\beta)^2 e^{\alpha\bar{b}} - (1-\beta)^2 e^{-\alpha\bar{b}}} \quad (4)$$

where i_0 is the incident intensity and $\bar{b}$ is the average cell path length for diffuse reflectance. It should be noted that, in order to obtain mathematically solvable equations, several simplifications were introduced in the original differential equations of Kubelka. These include insensitivity of the absorption/scattering coefficients to the light wavelength. In this regard, the corresponding coefficients in eq 1 should be regarded as effective ones. This simplification will not severely deteriorate the LIF predictions, since the intensity of the laser light is many orders of magnitude larger than that of the fluorescence. Thus, the main effects due to the presence of microparticles are attributed to the laser light absorption and scattering.

From the above equations, one can derive explicit equations for the transmitance, T (defined by $i_{(x=b)}/i_0$), and reflectance, R (defined by $j_{(x=0)}/i_0$):

$$T = \frac{4\beta}{(1+\beta)^2 e^{\alpha\bar{b}} - (1-\beta)^2 e^{-\alpha\bar{b}}}$$
$$R = \frac{(1-\beta^2)(e^{\alpha\bar{b}} - e^{-\alpha\bar{b}})}{(1+\beta)^2 e^{\alpha\bar{b}} - (1-\beta)^2 e^{-\alpha\bar{b}}} \quad (5)$$

Equations 5 are applied to obtain the final expression for the fluorescence in microparticle environment. The simplest expression for the fluorescence (ignoring the signal increase effect) would be proportional to the absorbed light, namely to $(1 - T - R)$, where T and R are a function of cell length b along the x coordinate. However, a portion of the scattered light is active along a perpendicular coordinate, directing to the detector. Equation 1 is now valid also for this portion of the scattered light, along the new coordinate. It means that the scattered light can be absorbed by fluorescing molecules (resulting in additional fluorescence), absorbed by microparticles, or rescattered. The same coefficients (ϵ_c, ϵ_m, ϵ_s) must hold for this process; however, a new effective cell length (d) must be assigned to allow for the experimental geometry in the perpendicular coordinate. Thus, equations similar to eq 5 can be obtained for that portion of the reflected light as well.

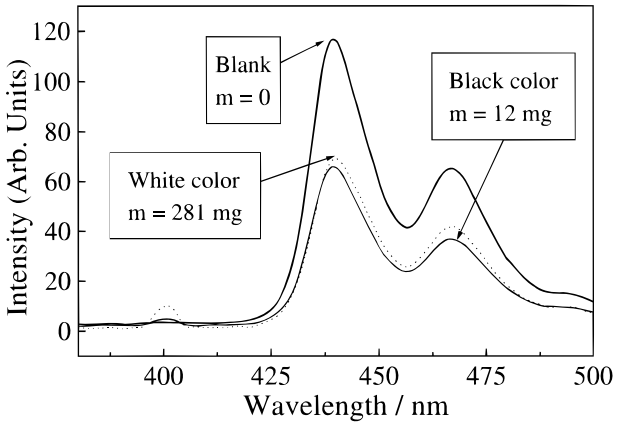

Figure 3. Perylene LIF spectra excited at 266 nm, in the presence of various microparticles.

In view of the above considerations, the approximated expression for the fluorescence in the presence of microparticles is

$$F = \frac{i_0 \epsilon_c C}{\epsilon_c C + \epsilon_m m}[(1 - T - R + \xi R(1 - T_d - R_d)] \quad (6)$$

where d designates that the corresponding expression is derived in the perpendicular coordinate and is a function of the effective cell length d in this direction, and ξ accounts for the fraction of the reflected light coupled into the detector coordinate. This equation provides a quantitative description of the space-integrated fluorescence originating from microparticle suspension solutions, in terms of the simple parameters: C, the concentration of the fluorescing agent; ϵ_c, the absorption coefficient of the fluorescing compound; ϵ_m, the absorption coefficient of the microparticles; m, their concentration; and ϵ_s, the scattering coefficient of the microparticles. Note that only a fraction of the absorbed light contributes to fluorescence, since a portion is absorbed by the microparticles. This is the origin of the prefactor in eq 6. This equation has been examined and compared to experimental data.

Experimental results were fitted to eq 6 by means of a nonlinear least-squares fitting program. This program was based on the Levenberg−Marquardt algorithm.[23] The fitting parameters included the scattering and the absorption coefficients, as well as ξ. This nonlinear fitting algorithm requires analytical differentiation of eq 6, with respect to all parameters. The expressions obtained for these derivatives are long and complicated and are not given here. The FORTRAN code of the function (eq 6) and all its derivatives are available upon request.

Experimental Results. Typical LIF data obtained upon irradiation at 266 nm by the Nd:YAG laser of 1.4 ppm perylene in clear acetonitrile (no externally incorporated particles) are shown in Figure 3. Such sets of data are, hereafter, referred either as *blank* or *reference* LIF signals. The fluorescence spectrum of perylene is characterized by a well-resolved double-peak structure between 425 and 475 nm.

Closely inspecting Figure 3, one finds that, with respect to their white counterparts (silica microparticulates), a quite comparable degree of signal reduction was produced by an almost 25 times

(23) Kortüm, G.; Oelkrug, Z. *Z. Naturforsch.* **1964**, *19a*, 28.

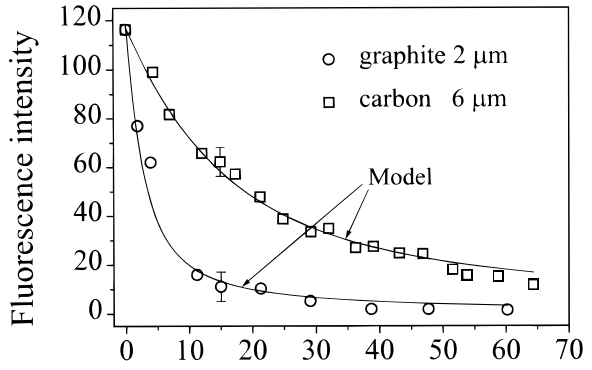

Figure 4. Fluorescence intensity as a function of microparticle added mass. The solid curve represents the theoretical model (eq 6).

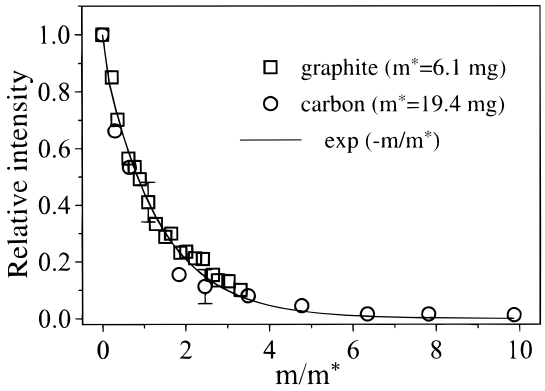

Figure 5. Rescaling of the data of Figure 4, producing a sample-independent fluorescence decay.

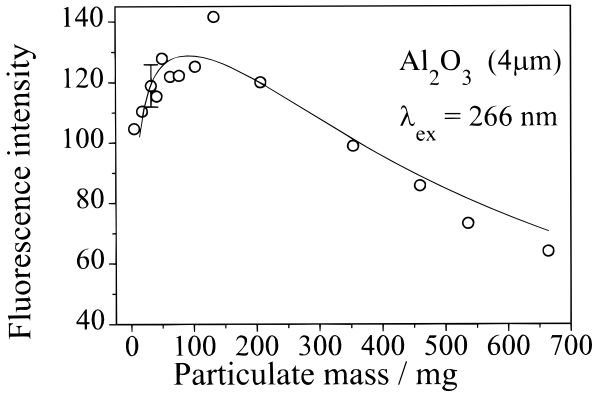

Figure 6. LIF signal increase in white-colored aluminum oxide microparticle suspension. The solid curve represents the theoretical model (eq 6).

smaller weight fraction of black microparticles (carbon). Such behavior could be anticipated in view of the more efficient light absorption properties of the latter.

Black-Colored Microparticle Suspensions. The fluorescence intensity as a function of the microparticle added mass is shown in Figure 4. Two particulate materials have been applied, graphite (2 μm) and carbon (6 μm), and both are shown on the same plot, together with the least-squares fitted eq 6. The graphite suspension system is characterized by a microparticle absorption coefficient of $\epsilon_m = 1.5$ and a scattering coefficient of $\epsilon_s = 0.002$. Clearly, the scattering coefficient of these black-colored particles is very small compared to the microparticle absorption coefficient.

Repeating the nonlinear fitting procedure for the carbon microparticle suspension provided the following results: $\epsilon_m = 0.28$ and $\epsilon_s = 0.002$. Again, the scattering coefficient is negligible. In this case, however, the microparticle absorption coefficient is ~5 times smaller. This number can be understood in terms of the difference between the particle sizes: assuming spherical particles of similar density, the ratio of the absorbing cross sections is inversely proportional to the particle diameters' ratio. In our case, this ratio is ~3. In view of the wide size distribution and the oversimplicity of our assumptions, this number can be considered in reasonable agreement with the ratio of absorption coefficients.

Inspection of the data of Figure 4 suggests that each matrix can also be characterized by an exponential decay coefficient. Thus, using a proper renormalization, one can find a compensation method for the microparticles effects on measured fluorescence. This method is expected to be valid as long as the scattering coefficients are negligible.

We present the data of Figure 4 in a normalized form, $I(m)/I(0)$; here, $I(0)$ is the respective blank signal spectral intensity. Each apparent exponential decay plot can be fitted as $\sim\exp(-\gamma m)$. Clearly, in such a case, a semilogarithmic type of calibration plots would consequently result. Hence we set γ to stand for the so-called, mass extinction coefficient of the media (suspension) for light-scattering/-absorbing processes.

In such a case, γ is expected to be a material-, laser wavelength-, particle size-, and particle size distribution-dependent parameter. Despite this, a simple mass coordinate renormalization procedure, with $m^* = 1/\gamma$, should be sufficient to produce a *sample-independent* exponential type calibration curve.

In this regard, for each type of black colored microparticles, the individual values of m^* were found by a least-squares fit of $\exp(-\gamma m)$ to the respective $I(m)/I(0)$ data. Rescaling m in terms of m^* produces $I(m/m^*)/I(0)$ of Figure 5, where m/m^* stands here for the renormalized mass coordinate.

When the data are plotted this way for different data sets (different black-colored microparticle powders), the similarity of the underlying physical properties for these types of suspensions is self-evident. Quite naturally, then, $\theta \approx 1$ should result for the repeated exponential fit, $\exp(-\theta m/m^*)$, to the combined $I(m/m^*)/I(0)$ data set.

Indeed, in support of the above, the best-fit procedure had produced $\theta = 0.8 \pm 0.2$. The solid line in Figure 5 represents, therefore, a *sample-independent* behavior, which was found to hold for the black-colored microparticle suspensions dealt with in the above.

White-Colored Microparticle Suspensions. Proceeding now to discuss the white-colored microparticle suspensions, we present first the detected LIF signals for perylene solutions with added aluminum oxide 4-μm particles, irradiated at 266 nm. The experimental points are shown in Figure 6. For small m, there is a well-resolved extremum in fluorescence intensity, corresponding to a sizable signal increase in LIF records. Equation 6 was fitted to these data, resulting in the solid curve in this figure. The best fitting parameters were $\epsilon_m = 0.000\,12$, $\epsilon_s = 0.248$, and $\xi = 0.79$. In this case, the microparticle's absorption is negligible when compared to the scattering.

The experimental results and the corresponding fit to eq 6, for fluorescence intensity in the presence of 3-μm silica particles

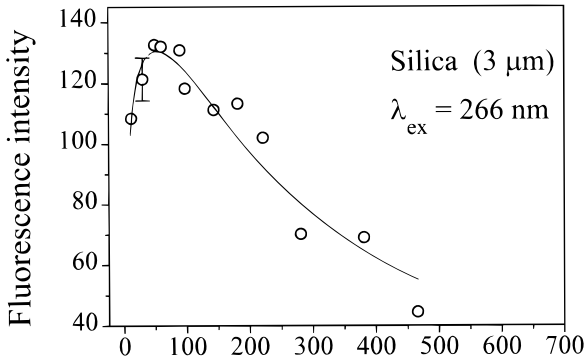

Figure 7. Perylene LIF intensity as a function of silica microparticle added mass. The solid curve represents eq 6, least-squares fitted to the experimental data. Excitation at 266 nm.

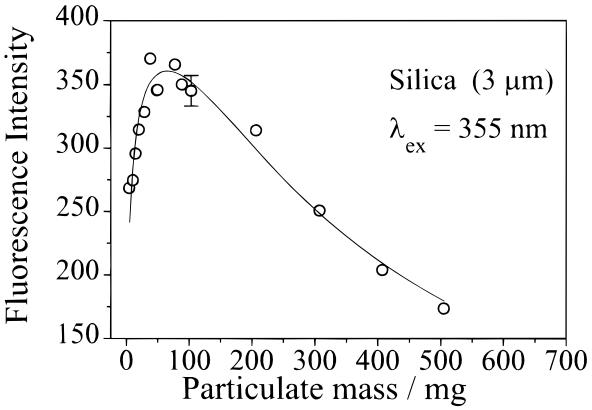

Figure 8. The same as in Figure 7, but excitation at 355 nm.

is presented in Figure 7. The best fitting parameters in this case were $\epsilon_m = 0.000\,45$, $\epsilon_s = 0.285$, and $\xi = 0.79$. Again, our model, in the form of eq 6, correctly reproduces the experimental data, both in the fluorescence maximum and in its decay. Also in this case, the microparticle absorption is negligible, and the scattering is predominant. The resulting scattering coefficient, however, is ~15% higher than that for aluminum oxide. This may be attributed, in part, to the larger overall cross section for the smaller average diameter of silica particles. The size factor is not fully implemented in the scattering coefficient ratio, due to the larger fractal dimension of the silica.

We have repeated the experimental measurements of fluorescence intensity as a function of added silica mass, at a different excitation wavelength. We irradiated with the third harmonic generation of our laser, at 355 nm. The experimental results are shown in Figure 8. As expected, higher fluorescence intensities are observed, corresponding to the higher laser energy at this wavelength. The solid curve represents our model (eq 6). The relevant fitting parameters were $\epsilon_m = 0.000\,31$, $\epsilon_s = 0.247$, and $\xi = 0.66$.

One can compare the results at the two wavelengths in terms of the effect on the light-scattering process. In this case, however, we are far from Rayleigh scattering predicting a λ^{-4} dependence characteristics: our particles are not very small compared to the incident wavelength but are not so large as to allow for the other limit. Thus, we can only apply the Kortüm−Oelkrug theory,[23] predicting $\epsilon_s \propto 1/\lambda^{\sigma}$, where $\sigma \approx 1$ for $(\bar{d}^2)^{1/2} \approx \lambda$ and $\sigma = 0 - 1$ for $(\bar{d}^2)^{1/2} > \lambda$. Examination of the two scattering coefficients obtained at 266 and 355 nm results in $\sigma = 0.5$, which is a reasonable figure.

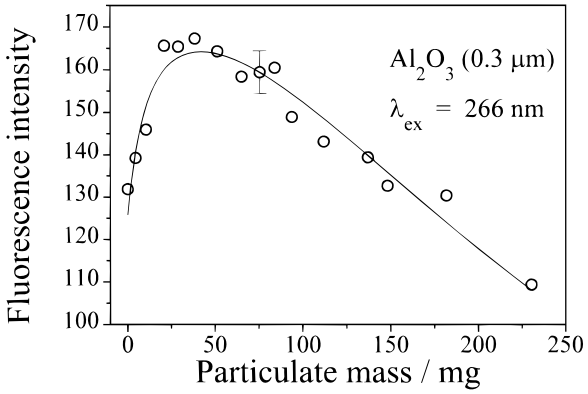

Figure 9. Particulate mass effect on perylene LIF in the presence of aluminum oxide. Excitation at 266 nm. The solid curve represents eq 6, least-squares fitted to the experimental data.

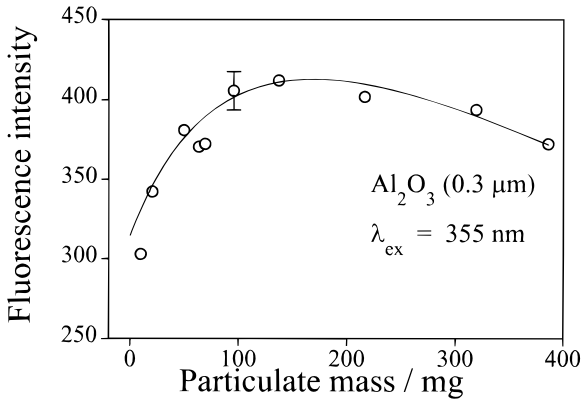

Figure 10. Same as in Figure 9, but excitation at 355 nm.

Finally, we measured the particulate mass effect on perylene fluorescence using aluminum oxide 0.3-μm particles at the two wavelengths of interest. The results at 266 and 355 nm are shown in Figures 9 and 10, correspondingly. The model was applied to these two cases. The best parameters describing the 266 excitation are $\epsilon_m = 0.001\,57$, $\epsilon_s = 0.126$, and $\xi = 0.6$, and for 355 excitation the figures are $\epsilon_m = 0.0012$, $\epsilon_s = 0.0115$, and $\xi = 0.68$. The model reproduces correctly the experimental data; however, the calculated γ value in this case is ~8, higher than expected by the Kortüm−Oelkrug theory.

It should be noted that larger values of m were found for the peak position corresponding to suspensions of larger particles. These findings were correctly accounted for by the model described in eq 6.

CONCLUSIONS

Laser-induced fluorescence (LIF) of acetonitrile solutions was studied here for different light-scattering/-absorbing microparticle matrixes. With increasing suspension mass, m, of efficiently light-absorbing, black-colored particles, the intensity of associated LIF signals (normalized to $m = 0$ data) was found to obey an exponential, ~exp($-\gamma m$), decrease. Their white-colored counterparts, however, initially produced a sizable, ~20%, signal increase of the respective LIF responses. Then, an exponential decrease became predominant. A model that assumes an effective scattering behavior of such white particle matrixes is developed. The overall suspension matrix-related effects on LIF data are reasonably well accounted for by this approach. It has been

shown that the effect of particle size distribution is correctly accounted for through their absorption and scattering coefficients. Other geometrical effects, such as the actual shape of the particles, are also accounted for in these coefficients.

An introduction of possible calibration algorithms is addressed. A "universal" particulates calibration plot was proposed for the high light-absorbtivity cases, while the calibration of light-emissive particles can be based on prior characterization of the three (scattering and absorption) coefficients involved. Real calibration work and the investigation of unknowns requires further investigation. Although it is hoped that this approach will eventually lead to direct LIF analysis of environmental samples (without filtration), this stage has not been achieved yet. This task should rely on accurate and detailed spectral acquisition, since several unknown parameters, including analyte concentration and the scattering/absorption coefficients of the particles, are to be simultaneously obtained using nonlinear least-squares fittings. Probably, additional information is necessary in real samples, and one may make use of the Rayleigh scattering peak or of simple absorption measurements. The incorporation of such data requires further development of the mathematical models describing the system of interest.

This research has covered only the full range limiting cases (white and black suspension particles). We intend to pursue investigating an "effective color chart" approach for unknown microparticle suspensions. The advantages offered by such charts are currently being studied in our laboratory.

ACKNOWLEDGMENT

This research was supported, in part, by the James-Franck Program for Laser Matter Interaction. V.V.G. and V.B. are grateful for financial support provided by the Israel Ministry of Absorption to returned citizens and/or new immigrant scientists.

Received for review January 14, 1998. Accepted April 29, 1998.

AC980046Z